Konrad-Zuse-Zentrum
für Informationstechnik Berlin

Takustraße 7
D-14195 Berlin-Dahlem
Germany

ILLIA HORENKO MARTIN WEISER

Adaptive Integration of Multidimensional Molecular Dynamics with Quantum Initial Conditions

ZIB-Report 02-29 (July 2002)

Adaptive Integration of Multidimensional Molecular Dynamics with Quantum Initial Conditions

Illia Horenko* and Martin Weiser

July 30, 2002

Abstract

The paper presents a particle method framework for resolving molecular dynamics. Error estimators for both the temporal and spatial discretization are advocated and facilitate a fully adaptive propagation.

For time integration, the implicit trapezoidal rule is employed, where an explicit predictor enables large time steps.

The framework is developed and exemplified in the context of the classical Liouville equation, where Gaussian phase-space packets are used as particles. Simplified variants are discussed shortly, which should prove to be easily implementable in common molecular dynamics codes. The concept is illustrated by numerical examples for one-dimensional dynamics in double well potential.

AMS MSC 2000: 81S30, 65J10, 65M99

Keywords: particle methods, adaptivity, error estimation, classical Liouville equation, molecular dynamics

*Freie Universität Berlin, Arnimallee 2, D-14195 Berlin, Germany, supported by DFG Sonderforschungsbereich 450

1 Introduction

The remarkable development of computer technology in recent time has led to a considerable progress in both theoretical studies and numerical simulations of molecular dynamics. The foundation of mathematical descriptions of molecular dynamics is provided by quantum theory in form of the time dependent Schrödinger equation. This partial differential equation, however, is defined on function spaces with a dimension proportional to the number of atoms. Already for medium size molecules, not to mention biomolecules, the curse of dimensionality leads to exponentially growing computational cost of traditional grid discretization techniques based on finite differences, finite elements, or the Fourier transform.

As a remedy for the curse of dimensionality, two alternatives to traditional grid discretization techniques are available: *sparse grids* (cf. [6]) and *particle methods* (cf. [14]), which all scale reasonably well to high dimensional problems.

Particle methods for solving the time dependent Schrödinger equation are often based on approximations to the equivalent Liouville-von-Neumann equation derived by means of the Wigner transformation, which casts the evolution into the phase space built of positions and momenta. The classical limit $\hbar \to 0$ of the Liouville-von-Neumann equation is called the *classical Liouville equation* (CLE), describing the dynamical behavior of a classical (quasi-)distribution function at constant energy in phase space.

The CLE can be discretized the by particle methods with different particle shape functions. A common approach is to approximate the phase space distributions by collections of Dirac functionals (cf. [17]). In this case, the dynamics is reduced to Newton's equations of motion, which are routinely solved in classical molecular dynamics simulations. The attractive simplicity of such a local particle base has, however, two major drawbacks. First of all, Dirac-functions representation is hardly applyable for problems where quantum effects and hence non-local effects in continuous distributions play an important role. In theses situations, which include non-adiabatic population exchanges [9], multi-dimensional potential energy surfaces with high barriers [13], and non-classical forces occurring in the "Bohmian" formulation of quantum mechanics [5], approximating the continuous Wigner distributions by collections of smooth particle shape functions is far more appropriate.Second, singular representation of continious quantum-mechanical distribution functions makes tedeous the on-fly error estimation and so far construction of time and space adaptive simulation algorithms. Typically the answer on this question is given in statistical Monte-Carlo sence requiring so far N^2 more particles in order to decrease error N times as it follows from the law of Large Numbers [16, 13, 1]. Strategy suggested in this paper is differnet in a way that combination of both singular and continious particles allows to control the *local* propagation error and so far generate new basis functions only there where it is needed.

For the numerical realization of a particle method for the CLE, two major tasks have to be performed: (i) the approximation of the initial Wigner distribution obtained from the initial quantum wave function by a collection of particle shape functions, and (ii) the propagation of the Wigner distribution in terms of the particle collection. Recently, Horenko, Schmidt, and Schütte [10] have proposed a particle method using *Gaussian phase space packets* (GPPs) introduced by Heller [7, 8, 3]. The initial Wigner distribution is constructed by a Monte Carlo sampling up to specified accuracy, whereas the propagation was performed by an explicit, symplectic integrator. Under the assumption of a locally quadratic potential, it has been shown that the propagation of a GPP yields again a GPP. For GPPs with sufficiently small diameter, the assumption of the potential being locally quadratic holds approximately. However, no error control for the propagation has been employed.

This work extends [10] by advocating an *adaptive propagation* using an implicit integrator with adaptively chosen step sizes, and an adaptive refinement of the GPP collection in case of non-quadratic potentials. The remainder of the paper is organized as follows. Section 2 is devoted to the time integration of the CLE dynamics by both implicit and explicit integrators, together with error control by adapting the time step size. In Section 3, the discretization of Wigner distributions by GPP collections is described, and the adaptive refinement of the approximation is presented. Finally, Section 4 contains numerical examples.

2 Time Integration of the CLE Dynamics

We consider the integration of linear time-dependent PDEs of the form

$$\partial_t \rho = \mathcal{L}\rho, \tag{1}$$

where $\rho : X \times \mathcal{R} \to \mathcal{R}^M$, $X = \mathcal{R}^N$, is a function to be propagated and the differential operator $\mathcal{L}$ has a purely imaginary spectrum. The framework we are presenting here is applicable to various situations, such as the Schrödinger equation or quantum-classical molecular dynamics. For the time being, however, we will concentrate on the classical Liouville equation

$$\begin{aligned} \partial_t \rho(R,P,t) &= -M^{-1}P^T \nabla_R\, \rho(R,P,t) \\ &\qquad + (\nabla_R\, V(R,t))^T \nabla_P\, \rho(R,P,t), \\ \partial_t \rho(R,P,0) &= \rho^0, \quad \forall R,P \end{aligned} \tag{2}$$

where the phase space consists of location R and impulse P, M is a diagonal matrix of masses, $V(R)$ is the potential energy function, and $\rho : \mathcal{R}^{n_{\mathrm{dim}}} \times \mathcal{R}^{n_{\mathrm{dim}}} \times \mathcal{R} \to \mathcal{R}$ is the Wigner quasi density.

As it has been already mentioned a number of approaches can be applied in order to integrate the partial differential equation (2). But all of the existing particle methods for the CLE, both with Dirac and Gauss functions as a basis share the lack of adaptivity in time and space. In order to construct such an adaptive method we employ the Rothe method [2] of semidiscretization in time, which leaves us with a stationary PDE to be solved in each time step. Spatial adaptivity can then be exploited for robust and efficient solution of these stationary problems.

Since the spectrum of the differential operator $\mathcal{L}$ is purely imaginary, Gauss methods seem to be suited best for time discretization. We choose the most simple scheme, the well-known trapezoidal rule

$$\Big(I - \frac{\tau}{2}\mathcal{L}\Big)\bar{\rho}(t+\tau) = \Big(I + \frac{\tau}{2}\mathcal{L}\Big)\rho(t), \tag{3}$$

which conserves first integrals. For the CLE this implies conservation of density and energy.

For adaptivity in time, we need three essential ingredients: an error estimator, a step size selection scheme, and an desired tolerance. In the following, we briefly recollect the standard methodology from integration of ODEs (cf. [4]).

Error estimator. Denoting the exact evolution by Φ, we estimate the unknown error

$$\epsilon := \|\bar{\rho}(t+\tau) - \Phi_\tau \rho(t)\| \tag{4}$$

by the difference between the trapezoidal rule and some comparison propagator ψ to be specified later:

$$[\epsilon] := \|\bar{\rho}(t+\tau) - \Psi_\tau \rho(t)\|. \tag{5}$$

In case $[\epsilon] \leq \mathrm{TOL}$ the step is accepted, otherwise we reduce the step size and repeat the step.

Step size selection scheme. Since the trapezoidal rule is of second order, we assume the error propagation model

$$\epsilon \approx C\tau^3 \tag{6}$$

to hold locally for some slowly varying constant C. Substituting $[\epsilon]$ for ϵ and aiming at an error of $\sigma\mathrm{TOL}_t$ with some safety factor $\sigma < 1$, we obtain an optimal step size

$$\tau_{\mathrm{opt}} = \sqrt[3]{\frac{\sigma\mathrm{TOL}_t}{[\epsilon]}}\,\tau, \tag{7}$$

that is used for the next step or recomputing the current time step, respectively.

Tolerance. The tolerance TOL is usually assumed to be an accuracy requirement provided by the user. As will be worked out in Section 2, the spatial discretization by a particle method leads to an additional tolerance requirement.

3 Adaptive Phase Space Discretization

For approximating the distributions to be propagated, we use a linear combination

$$\rho(t) = \sum_{n=1}^{N} B_n(t) g(x_n(t), G_n(t)) \tag{8}$$

of particles g positioned at points $x_n(t)$ in space. Additionally, the shape of the particles is allowed to depend on a set of shape parameters $G_n(t)$.

For the CLE, we use Gaussian phase space packets (GPP's) defined as

$$g(\bar{R}, \bar{P}, \bar{G})(R, P) := \exp\left[- \begin{pmatrix} R - \bar{R} \\ P - \bar{P} \end{pmatrix}^T \bar{G} \begin{pmatrix} R - \bar{R} \\ P - \bar{P} \end{pmatrix} \right], \tag{9}$$

where the shape matrix $\bar{G} \in \mathcal{R}^{4n_{\dim}^2}$ is symmetric positive definite.

In order to propagate an initial Wigner density by means of the particle discretization given above, two tasks have to be tackled. First an initial GPP approximation of a given Wigner density has to be computed, and second, in every time step a new GPP approximation to the exact propagation of the current GPP approximation must be found.

3.1 Initial GPP approximation

A method to approximate a given Wigner density ρ_0 by a small set of GPP's has been recently proposed by Horenko, Schmidt, and Schütte [10]. Since similar techniques are developed in Section 3.2 for spatial adaptivity, we sketch the method here for convenience.

The aim is to achieve a sufficiently small spatial approximation error

$$\Big\| \rho_0 - \rho(0) \Big\|_{\mathcal{L}_1} \leq \mathrm{TOL}_x$$

subject to G_n symmetric positive definite with some number N of GPP's to be determined as small as possible. In order to make the task computationally tractable, we substitute the $\mathcal{L}_1$-norm by a discrete sampling at K_N points and simplify the positive definiteness constraint to fixing $G_n = \lambda I$ with some $\lambda > 0$, obtaining the requirement

$$\|\rho_0 - \rho(0)\|_{\{R_k, P_k\}} := \sum_{k=1}^{K_N} \omega_k \Big| \rho_0(R_k, P_k) - \rho(R_k, P_k, 0) \Big|^2 \leq \mathrm{TOL}_x. \tag{10}$$

For (10) to be sufficiently accurate we have to select at least as many sample points as the representation (8) has degrees of freedom, and hence require $K_N \geq N(1 + 2n_{\text{dim}})$. For fixed N, the approximation error can be minimized by a Gauss-Newton method. Initial centers $(\bar{R}_n, \bar{P}_n)$ of the GPP's and sampling points (R_k, P_k) are obtained by a Monte-Carlo sampling of the regions of phase-space where the absolute value of the quasi–probability density ρ_0 exceeds a certain threshold. For simplicity, we include the GPP's centers into the set of sampling points by setting $(R_k, P_k) = (\bar{R}_n, \bar{P}_n)$ for $1 \leq k \leq N$ and generate at least $2Nn_{\text{dim}}$ more sampling points by the same Monte-Carlo process. In concordance with the probabilistic density of the sampling points, the weights have to be chosen as

$$\omega_k := \frac{\|\rho_0\|_{\mathcal{L}_1}}{K_N \rho_0(R_k, P_k)}.$$

If the local optimum computed by the Gauss-Newton method does not satisfy (10), N is increased and additional GPP's are created by Monte-Carlo sampling. The process is then repeated until the accuracy requirement is fulfilled.

Simplifications. Several computational simplifications are possible and will be convered in more detail in a subsequent paper [11]. First we may fix the GPP's' centers $(\bar{R}_n, \bar{P}_n)$ and perform the minimization with respect to the amplitudes B_n only, which reduces the nonlinear approximation problem to a linear least squares problem:

$$\|SB - W\|_2 = \min, \tag{11}$$

where $S_{kn} = g(\bar{R}_n, \bar{P}_n, \bar{G}_n)(R_k, P_k)$ and $W_k = \rho(R_k, P_k, 0)$. In this case, we require only $K_N \geq N$ sample points. It can be expected, however, that a larger number N of GPP's is necessary to satisfy (10).

In general, the system matrix S is dense due to the global support of the GPP's. Nevertheless, most of the entries will be very small due to the GPP's exponential decay. Dynamically sparsing the system matrix therefore enables the application of efficient sparse matrix algorithms to solve the least squares problem.

It is noted that the linear problem (11) may become numerically ill–conditioned for a large number of wide GPP's, whenever the function to be approximated significantly oscillates on length scales comparable to the width of the GPP's. However, this does not pose a severe problem since (a) it can be monitored by computing the condition number of matrix S, and (b) we can avoid the problem by reducing the widths of the GPP's.

Choosing $K_N = N$ and the sample points (R_i, P_i) identical to the centers $(\bar{R}_i, \bar{P}_i)$, the least squares problem is simplified to a system of equations. The approximation quality, however, may be less robust.

3.2 Propagation of GPP approximations

Inexact propagation. The propagation of the Wigner density ρ by the implicit trapezoidal rule (3) poses an approximation problem similar to that encountered in Section 3.1, namely to find a new density $\rho(t+\tau)$ representable by GPP's such that

$$\left\| \left(I - \frac{\tau}{2}\mathcal{L}_c\right)\rho(t+\tau) - \left(I + \frac{\tau}{2}\mathcal{L}_c\right)\rho(t) \right\|_{\mathcal{L}_1} \leq \mathrm{TOL}_x \tau^3. \tag{12}$$

The factor τ^3 is necessary in order not to destroy the second order convergence of the trapezoidal rule.

By sampling at K points (R_i, P_i), we again reduce (12) to a computationally tractable nonlinear least squares problem

$$\left\| \left(I - \frac{\tau}{2}\mathcal{L}_c\right)\rho(t+\tau) - \left(I + \frac{\tau}{2}\mathcal{L}_c\right)\rho(t) \right\|_{\{R_k, P_k\}} \leq \mathrm{TOL}_x \tau^3 \tag{13}$$

with K_N non-linear equations and $N(1+2n_{\mathrm{dim}})$ unknowns B_n, $\bar{R}_n$, and $\bar{P}_n$ defining $\rho(t+\tau)$.

Fortunately, the costly Monte-Carlo generation of the centers $(\bar{R}_n, \bar{P}_n)$ can be omitted here due to the continuity of the evolution: Since for sufficiently small time steps τ the new density $\rho(t+\tau)$ is close to the old one, we can expect that the Gauss-Newton method starting at the old density $\rho(t)$ converges quickly towards the closest local minimum of the approximation error (13).

For larger stepsizes τ, the Gauss-Newton method may converge slowly and possibly towards a different local minimum. For efficiency and robustness reasons, we therefore suggest to limit the stepsize τ such that the Gauss-Newton method satisfies the accuracy requirement (13) after the first step.

Another question which has to be addressed is the choice of sample points (R_i, P_i), $i = 1, \ldots, K_N$. For the least squares problem (13) not to be underdetermined, we require at least $K_N \geq N(1+2n_{\mathrm{dim}})$ sample points, preferably distributed in accordance with the quasi-probability density $\rho(t)$. Since performing a Monte-Carlo sampling at every time step is prohibitively expensive, we suggest to select the sampling points from the initial GPP approximation outlined in Section 3.1 for the first time step at $t = 0$. For subsequent steps, we suggest to take again the centers of the GPP's, i.e. $(R_i(t+\tau), P_i(t+\tau)) = (\bar{R}_i(t+\tau), \bar{P}_i(t+\tau))$, $i = 1, \ldots, N$, and additionally the remaining sampling points from the previous step propagated in time as Dirac pulses by the CLE, i.e. $(R_i(t+\tau), P_i(t+\tau)) = \Phi_\tau(R_i(t), P_i(t))$, $i = N+1, \ldots, K_N$. Due to their nonoverlapping support, such Dirac pulses can be propagated efficiently and independently of each other by the Hamiltonian dynamics (16)–(17) below (see [10]).

Spatial adaptivity. It may happen that the number N of GPP's is too small, such that the accuracy requirement (13) cannot be satisfied. In this case, as few as possible additionall GPP's have to be created in order to reduce the approximation error sufficiently. Fortunately, the local residuals

$$\epsilon_k = \Big| \Big(I - \frac{\tau}{2}\mathcal{L}\Big)\rho(R_k, P_k, t+\tau) - \Big(I + \frac{\tau}{2}\mathcal{L}\Big)\rho(R_k, P_k, t) \Big| \tag{14}$$

provide a useful local error indicator suitable for extending the particle set. The following scheme is intended to insert the new particles at positions in phase-space, where the approximation error is largest, and hence to improve the approximation at a small cost.

Assume the sample points $k = N+1, \ldots, K_N$ are sorted ascendingly by their local residual $\omega_i \epsilon_k$. Let $j > N$ be maximal such that

$$\sum_{k=1}^{j} \omega_i \epsilon_i \leq \mathrm{TOL}_x \tau^3 \tag{15}$$

holds, or $j = N$ if (15) cannot be satisfied. We then suggest to substitute (or "upgrade") the sample points $j+1, \ldots, K_N$ by newly created GPP's with centers (R_k, P_k), $k = j+1, \ldots, K_N$, amplitude zero, and shape matrix λI, and create at least $2n_{\mathrm{dim}}(K_N - j)$ new sample points in the vicinity of the newly created GPP's by some Monte-Carlo method. N and K_N should be increased accordingly, and the sampling points should be sorted such that again the first N correspond to the centers of the GPP's.

With the enlarged particle set at hand, the Gauss-Newton step is performed again in order to meet the requirement (13). If necessary, the adaptive refinement is repeated until finally (13) is met.

Asymptotic conservation properties. The adaptive refinement scheme described above recovers the conservation of energy and volume featured by the exact trapezoidal rule (3) asymptotically for $\mathrm{TOL}_x \to 0$. Assuming the potential V to be bounded, differences of the energy

$$\langle E, \rho \rangle = \int \big(V(R) + \frac{1}{2} P M^{-1} P^T\big)\rho \, dP dR$$

is a continious linear functional due to the exponential decay of the GPP's representing ρ.

Since the exact trapezoidal rule conserves quadratic first integrals, the energy error of the approximate solution $\rho(t+\tau)$ satisfying (13) can be bounded by

$$
\begin{aligned}
\epsilon_E(t) &:= |\langle E, \rho(t+\tau) - \Phi_\tau \rho(t)\rangle| \\
&\leq |\langle E, \rho(t+\tau) - \bar{\rho}(t+\tau)\rangle| + \underbrace{|\langle E, \bar{\rho}(t+\tau) - \Phi_\tau \rho(t)\rangle|}_{=0} \\
&\leq \|E\| \, \|\rho(t+\tau) - \bar{\rho}(t+\tau)\|_{\mathcal{L}_1} \\
&\leq \|E\| \, \big\|\big(I - \frac{\tau}{2}\mathcal{L}\big)^{-1}\big\| \, \big\|\big(I - \frac{\tau}{2}\mathcal{L}\big)(\rho(t+\tau) - \bar{\rho}(t+\tau))\big\|_{\mathcal{L}_1} \\
&\leq \|E\| \, \big\|\big(I - \frac{\tau}{2}\mathcal{L}\big)\rho(t+\tau) - \big(I + \frac{\tau}{2}\mathcal{L}\big)\rho(t))\big\|_{\mathcal{L}_1} \\
&\leq \|E\| \, \mathrm{TOL}_x \tau^3.
\end{aligned}
$$

Here we have used that the differential operator $\mathcal{L}$ has an unbounded, purely imaginary spectrum, which implies $\|(I - \frac{\tau}{2}\mathcal{L})^{-1}\| = 1$.

Analogously, asymptotic conservation of volume can be shown, or, for different evolutions, conservation of arbitrary quadratic first integrals.

Note that this result does not guarantee long term conservation of energy, as has been established for the method of lines, i.e. semidiscretization in space, by Hairer, Lubich, and Wanner et al. [12].

Explicit Predictor. The simplest choice of the starting point for the Gauss-Newton method is of course the current GPP collection $\rho(t)$. However, since $\rho(t+\tau) - \rho(t) = \mathcal{O}(\tau)$, the time step τ is limited by the requirement that the initial guess should be sufficiently good such that the local Gauss-Newton iteration converges quickly and reliably to the nearest local solution — see Figure 4.

The employment of a cheaply computable predictor providing a better initial guess can be expected to relax this additional restriction considerably, and hence can lead to larger time steps.

For the CLE considered here we suggest to use an explicit symplectic modified Leap-Frog propagator Ψ recently proposed by Horenko, Schmidt, and Schütte [10] as predictor.

In the simple case of a quadratic (or harmonic) potential, the Gauss-particles in the ensemble can be propagated independently with evolution equations for the parameters R_n, P_n, and G_n derived from (2):

$$\partial_t R_n = M^{-1} P_n \tag{16}$$

$$\partial_t P_n = -\nabla_R V(R_n) \tag{17}$$

$$\partial_t \mathbf{G}_n = \mathbf{C}(R_n)\mathbf{G}_n + \mathbf{G}_n \mathbf{C}^T(R_n), \tag{18}$$

where

$$C(R_n) = \begin{pmatrix} 0 & \nabla_R^2(R_n) \\ -M^{-1} & 0 \end{pmatrix}.$$

For sufficiently small GPP's, general potentials are locally almost quadratic, such that the predictor solution $\Psi_\tau\rho(t)$ can be expected to provide a good approximation of the exact solution $\Phi_\tau\rho(t)$.

Having the predictor solution $\Psi_\tau\rho(t)$ at hand, it can also be used as comparison evolution for the error estimator (5) of the time discretization. As a computational simplification we suggest to use the following modification of (5):

$$\begin{aligned}[\epsilon(t+\tau)] &= \left\| \Big(I - \frac{\tau}{2}\mathcal{L}\Big)(\bar{\rho}(t+\tau) - \Psi_\tau\rho(t)) \right\|_{\{R_k,P_k\}} \\ &= \left\| \Big(I - \frac{\tau}{2}\mathcal{L}\Big)\Psi_\tau\rho(t) - \Big(I + \frac{\tau}{2}\mathcal{L}\Big)\rho(t) \right\|_{\{R_k,P_k\}}, \end{aligned} \tag{19}$$

which is just the initial Gauss-Newton residual.

Algorithm 1.

Initial phase-space distribution approximation (GPP decomposition):

$N := \mathrm{TOL}_x^{-1/2}$
direct Monte-Carlo generation of $(\bar{R}_n, \bar{P}_n), n = 1, \ldots, N$
$K_N := 2Nn_{\mathrm{dim}}$
direct Monte-Carlo generation of $(R_k, P_k), k = 1, \ldots, K_N$
solve nonlinear approximation problem (10) for $B_n, \bar{R}_n, \bar{P}_n$
while $\|\rho_0 - \sum_{n=1}^{N} B_n g(\bar{R}_n, \bar{P}_n, \lambda I)\|_{\{R_k,P_k\}} > \mathrm{TOL}_x$:
  $N := 1.1N$
  $K_N := 2Nn_{\mathrm{dim}}$
  direct Monte-Carlo generation of new GPP's and sample points
  solve nonlinear approximation problem (10) for $B_n, \bar{R}_n, \bar{P}_n$

Inexact propagation of GPP distribution:

while $t < T$:
  compute predictor $\Psi_\tau\rho(t)$
  compute error estimator $[\epsilon]$ from (19)
  solve nonlinear approximation problem (13) for $B_n, \bar{R}_n, \bar{P}_n$
  while (13) not satisfied:
    $N := K_n - j$ with j from (15)
    $K_N := 2Nn_{\mathrm{dim}}$
    local generation of new GPP's and sample points
    solve nonlinear approximation problem (13) for $B_n, \bar{R}_n, \bar{P}_n$
  $t := t + \tau$
  $\tau := \sqrt[3]{\sigma \mathrm{TOL}_t/[\epsilon]}\,\tau$

4 Numerical Example

As an example for the application of the proposed dynamical scheme we consider a one-dimensional model of the Gauss-shaped density initially centered at 0.5 a.u. of length with width parameter 0.5 and momentum 30 a.u. in a double well potential (Fig. 1). This model can for example describe the proton-transfer process in proteins or liquids.

Three different approaches to the numerical solution of the CLE (2) are compared: the explicit GPP approach (16-18), the inexact implicit trapezoidal rule (3), and a grid-based method [15] (512×512 points) where the partial derivatives are evaluated by means of the fast Fourier transform and the time propagation is performed by means of a split operator scheme. The initial Wigner density is decomposed into an ensemble of GPP's with global error of 5%. Fig. 2 shows position representations of the density evolution on a time-span of 7.5 fs as obtained from the grid-based (solid line), explicit (dotted line), and implicit (crosses) methods. The visible deviation of the explicit propagator on one hand from the grid and implicit integrators on the other hand is attributed to the violation of the locally quadratic approximation in the course of propagation.

Fig. 3 illustrates the influence of particle width on the predictor result quality in the adaptive algorithm. The difference between the two curves can again be explained by the violation of the locally quadratic approximation. The deterioration of the locally quadratic approximation is caused by both the GPPs getting wider and being propagated into spatial regions with a higher nonlinearity of the potential's gradient.

Another numerical example shows the efficiency of the space-adaptive algorithm (Fig. 4). Difference between predictor-corrector propagation without space-adaptivity (dotted line) and adaptive predictor-corrector propagation illustrates the fact that growing inefficiency of modified Leap-Frog predictor (explained with spreading of GPP's during the propagation) can be compensated by local upgrading of Dirac points to GPPs as explained in Section 3.2.

Fig. 5 displays the total energy conservation for explicit (10 GPP's dashed and 100 GPP's dotted line) and implicit propagation (10 GPP's circles and 100 GPP's dash-dotted line). Deviations from a constant level in both cases are due to an insufficient number of particles in the ensemble when the exact trapezoidal equation (3) is substituted by its approximate analog (13).

Acknowledgement. The authors would like to thank Ch. Schütte for helpful suggestions, and W. Huisinga and B. Schmidt for careful reading of the manuscript.

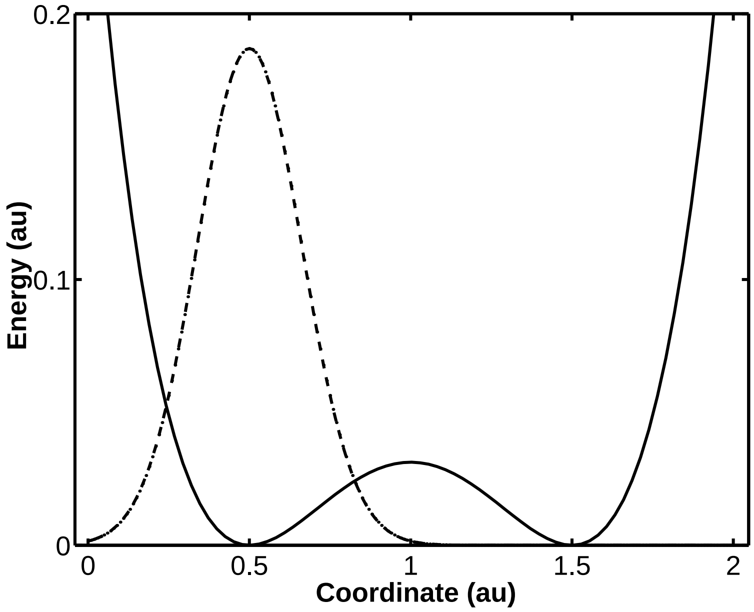

Figure 1: Potential energy surface $V(R)$ and initial Wigner density in position representation.

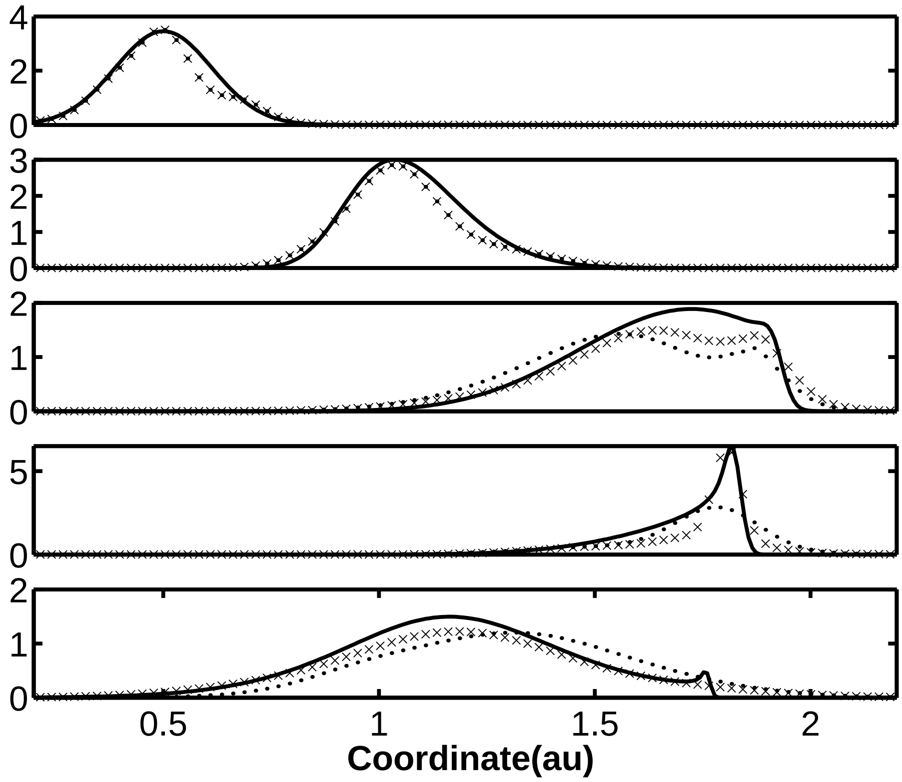

Figure 2: Snapshots of position space representation of the Wigner density evolution at times 0, 1.875, 3.75, 5.625, 7.5 fs as obtained from the grid-based (solid line), modified Leap-Frog (dotted line), and adaptive (crosses) methods.

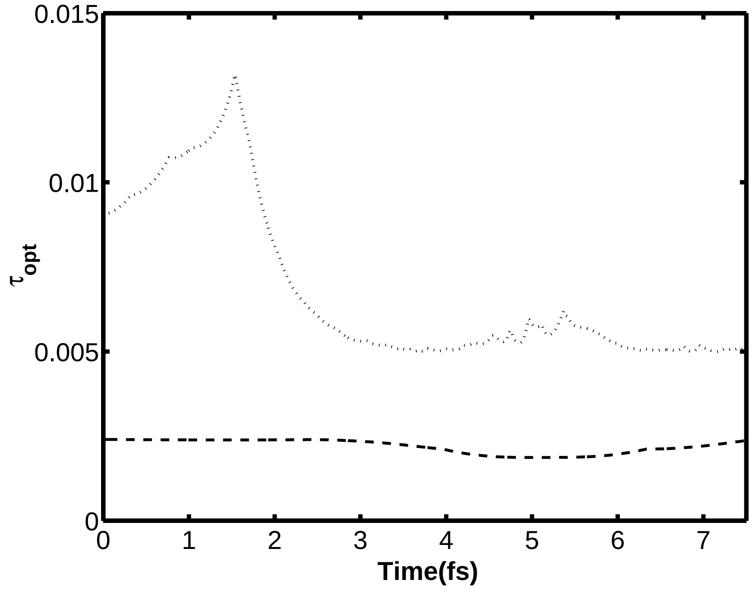

Figure 3: Optimal time step of the predictor-corrector scheme without spatial adaptivity as function of time for a decomposition of the initial density into 10 wide GPP's (dashed) and 100 narrow GPP's (dotted).

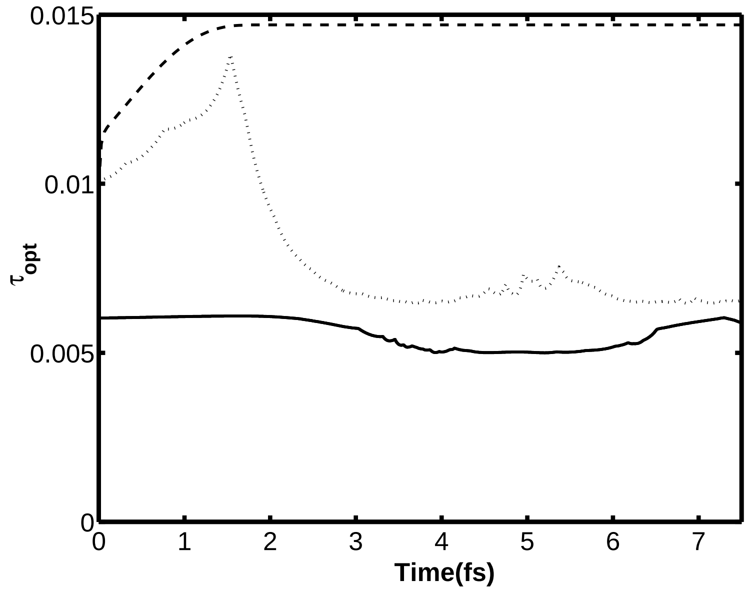

Figure 4: Optimal time-step for a propagation without predictor (solid), with modified Leap-Frog second order predictor (dotted) without phase-space adaptivity, and fully adaptive predictor-corrector scheme (dashed) for 100 initial GPP's.

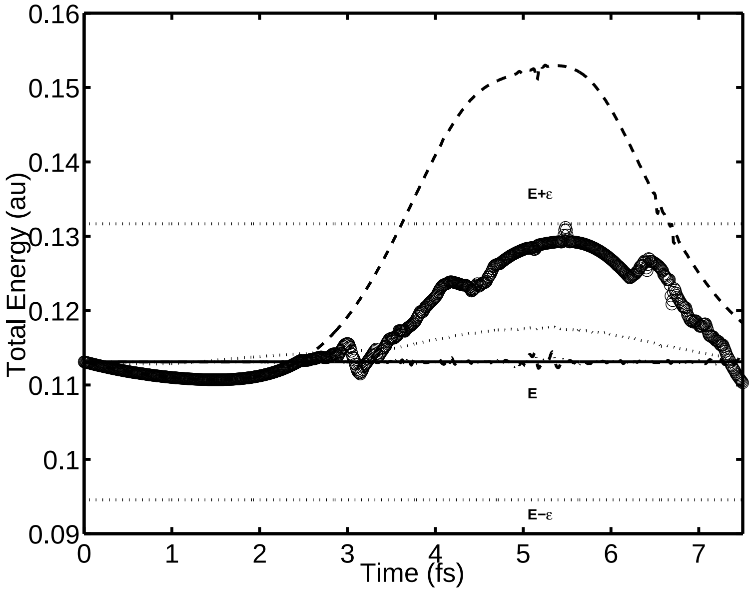

Figure 5: Total energy conservation by a global allowed energy error $\epsilon_E = n_{\mathrm{steps}} \sup\{\epsilon_E(t)\} = 0.18$ in the case of modified Leap-Frog for 10 (dashed) and 100 (dotted) initial GPP's compared with the proposed adaptive predictor-corrector scheme for 10 (circles) and 100 (dash-dotted line) initial GPP's.

References

[1] A. Arnold and F. Nier. Numerical analysis of the deterministic particle method applied to the wigner equation. *Mathematics of Computation*, 58:645–669, 1992.

[2] F. Bornemann. An adaptive multilevel approach to parabolic equations I. general theory and 1d-implementation. *IMPACT Comput. Sci. Eng.*, 2:279–317, 1990.

[3] R. C. Brown and E. J. Heller. Classical trajectory approach to photodissociation: The Wigner method. *J. Chem. Phys*, 75:186–188, 1981.

[4] P. Deuflhard and F. Bornemann. *Scientific Computing with Ordinary Differential Equations*. Springer, 2002.

[5] A. Donoso and C. C. Martens. Quantum tunneling using entangled classical trajectories. *Phys. Rev. Lett.*, 87(22):202–223, 2001.

[6] M. Griebel and G. Zumbusch. Adaptive sparse grids for hyperbolic conservation laws. In Michael Fey, editor, *Hyperbolic problems: Theory, numerics, applications.Proceedings of the 7th international conference,Zürich, Switzerland, February 1998.*, volume 1 of *Int. Ser. Numer. Math.129*, pages 411–422. Basel: Birkhäuser, 1999.

[7] E. J. Heller. Time–dependent approach to semiclassical dynamics. *J. Chem. Phys.*, 62(4):1544–1555, 1975.

[8] E. J. Heller. The semiclassical way to molecular spectroscopy. *Acc. Chem. Res.*, 14:368–375, 1981.

[9] I. Horenko, Ch. Salzmann, B. Schmidt, and Ch. Schütte. Quantum–classical Liouville approach to molecular dynamics: Surface hopping Gaussian phase–space packets. *J. Chem. Phys., submitted*, 2001.

[10] I. Horenko, B. Schmidt, and Ch. Schütte. Multidimensional classical Liouville dynamics with quantum initial conditions. *J. Chem. Phys., submitted*, 2001.

[11] I. Horenko and M. Weiser. Extending classical molecular dynamics codes to particle methods using frozen gaussian phase-space packets (in preparation).

[12] E. Hairer, Ch. Lubich, and G. Wanner. *Geometric Numerical Integration*. Springer, 2002.

[13] J. Ma, D. Hsu, and J. E. Straub. Approximate solution of the classical Liouville equation using Gaussian phase packet dynamics: Application

to enhanced equilibrium averaging and global optimization. *J. Chem. Phys.*, 99(5):4024–4035, 1993.

[14] H. Neunzert, A. Klar, and J. Struckmeier. Particle methods: Theory and applications. In K. Kirchgaessner, editor, *ICIAM 95: proceedings of the Third International Congress on Industrial and Applied Mathematics held in Hamburg, Germany*, 1995.

[15] G. Strang. On the construction and comparison of difference schemes. *SIAM J. Numer. Anal.*, 5:506–517, 1968.

[16] K. Takahashi. Distribution functions in classical and quantum mechanics. *Progr. Theor. Phys. Suppl.*, 98:109–156, 1989.

[17] E. P. Wigner. On the quantum correction for thermodynamic equilibrium. *Phys. Rev.*, 40:749–759, 1932.